Sensors & Transducers, Vol. 27, Special Issue, May 2014, pp. 87-91

www.sensorsportal.com

Sensors & Transducers

http://www.sensorsportal.com

Characterization and Modeling I(V) of the Gate Schottky Structures HEMTs Ni/Au/AlInN/GaN

[1] N. BENYAHYA, [1] H. MAZARI, [1] N. BENSEDDIK, [1] Z. BENAMARA, [1] M. MOSTEFAOUI, [1] K. AMEUR, [1] R. KHELIFI, [2] J. M. BLUET, [2] W. CHIKHAOUI, [2] C. BRU-CHEVALLIER

[1] Laboratoire de Microélectronique Appliquée, Département d'électronique, Université Djillali Liabès de Sidi Bel-Abbes, 22000 Sidi Bel-Abbes, Algérie

[2] Université de Lyon, Institut des Nanotechnologies de Lyon, INL-UMR5270, CNRS, INSA de Lyon, Villeurbanne F-69621, France

[1] Tel.: +213 48551284, fax: +213 48551284

[1] E-mail: benyahya22@hotmail.fr

Received: 31 December 2012 /Accepted: 10 August 2013 /Published: 26 May 2014

Abstract: In this paper, we have studied the Schottky contact of Ni/Au/AlInN/GaN HEMTs. The current–voltage Igs (Vgs) of Ni/Au/AlInN/GaN structures were investigated at room temperature. The electrical parameters such as ideality factor (2.3), barrier height (0.72 eV) and series resistance (33 Ω) were evaluated from I(V) data, the threshold voltage (-2.42 V), the 2D gas density (1.35×10^{13} cm^{-2}) and barrier height (0.94 eV) were evaluated from C(V) data. *Copyright © 2014 IFSA Publishing, S. L.*

Keywords: GaN, AlInN, Electrical characterization, HEMT transistor.

1. Introduction

In recent years AlInN semiconductor layer have been extensively studied and used in semiconductor devices like high electron mobility transistor (HEMTs) because of their excellent performances in high frequency and high power [1, 2]. AlInN was proposed by Kuzmík as an alternative lattice matched barrier for GaN-based HEMTs [3], AlInN/GaN HEMTs have been reported to show a remarkable stability by surviving operation at temperatures as high as 1000 °C [4]. In this paper, we report a characterization and modeling I(V) of the gate Schottky structures HEMTs AlInN/GaN.

2. Technology

The Ni/Au/AlInN/GaN HEMT was fabricated by Low Pressure Metal Organic Chemical Vapour Deposition (LPMOCVD) on SiC substrates. The epitaxial structure is composed of a buffer layer, an undoped GaN layer, and an undoped $Al_{0.82}In_{0.18}N$ barrier layer deposited on the top of an AlN spacer. The ohmic contacts are Ti/Al/Ni/Au stacks deposited by evaporation followed by an annealing at 900 °C for 30 s under Nitrogen atmosphere. Schottky contacts of the gate were carried out by Ni/Au bilayer evaporation. The device is passivated with SiN using plasma enhanced chemical vapor deposition. Fig. 1 shows the structure of Ni/Au/AlInN/GaN HEMT.

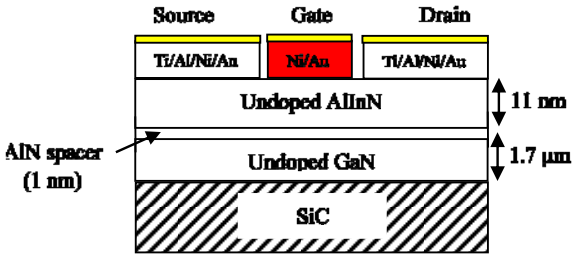

Fig. 1. Structure of AlInN/GaN HEMT.

The technological properties of the structure studied are tabulated in Table 1.

Table 1. The technological properties of the HEMT.

Substrate	SiC
Buffer layer thickness	GaN (1.7 μm)
Schottkylayerthickness	AlInN (11 nm)
Spacer layerthickness	AlN (1 nm)
x (of Al (%))	82
Ohmic contact	Ti/Al/Ni/Au
Gate contact	Ni/Au
Passivation	SiN

The dc measurements were carried out using an HP4155B semiconductor parameter analyzer and the measurements of capacitance with measuring instrument "Keithley Test System" at high frequency 1 MHz.

3. Method of Analysis

When a metal–semiconductor (MS) contact with an interfacial layer is considered, it is assumed that forward bias current in a Schottky barrier is due to thermionic emission current I_{TE} corrected by tunneling, which is expressed as [5]:

$$I = I_{TE0} \exp\left(\frac{qV}{nkT}\right), \tag{1}$$

$$I_{TE0} = SA \times T^2 \exp\left(-x^{0.5}\delta\right)\exp\left(-\frac{q\phi_{bn}}{kT}\right), \tag{2}$$

The semi-Ln(I) curve gives by extrapolation up to zero voltage the current of saturation I_{TE0}.

A^*: Richardson constant (120(m_{*n}/m_0)); S: diode area; T: temperature; m_n^*: effective mass of the electron; m_0: free electron mass; δ: interfacial layer thickness; x mean barrier height presented by the thin interfacial layer; k: Boltzmann constant; q: electrical charge; n: ideality factor; ϕ_{bn} barrier height.

As a refinement of this method the series resistance R_s and the ideality factor n were introduced to include the contribution of other current transport mechanisms. Then:

$$I = I_{TE0}\left\{\exp\left(\frac{qV - R_s I}{nkT}\right) - 1\right\}, \tag{3}$$

R_s depends on the thickness epitaxial layer, the doping concentration and the electron mobility [6].

The Currents existing in the structure are determined by different physical phenomena such as thermionic emission (I_{TE}), the generation-recombination (I_{GR}), tunneling (I_{TU}) and leakage current (I_{LK}), and the total current may be given by the following relationship

$$I_{tot} = I_{TE} + I_{GR} + I_{TU} + I_{LK}, \tag{4}$$

The thermionic emission component of the current is:

$$I_{TE} = I_{TE0}\left\{\exp\left(\frac{qV - R_s I}{kT}\right) - 1\right\}, \tag{5}$$

where I_{TE0} is the saturation value of the thermionic current component I_{TE}; R_S is the series resistance, and I is the total current. Note that writing Eq. 5 it has been assumed that the ideality factor n=1. This is necessary because one takes into account the generation-recombination current I_{GR}, the tunneling current I_{TU} and leakage current I_{LK}.

The generation-recombination component of the current is:

$$I_{GR} = I_{GR0}\left\{\exp\left(\frac{qV - R_s I}{2kT}\right) - 1\right\}, \tag{6}$$

where I_{GR0} is the saturation value of the generation-recombination component I_{GR}, with:

$$I_{GR} = \frac{qSWn_i}{2\tau}, \tag{7}$$

where W is the depletion width, n_i is the intrinsic carrier concentration, S is the diode area and τ is the carrier lifetime.

The tunneling component of the current is:

$$I_{TU} = I_{TU0}\left\{\exp\left(\frac{qV - R_s I}{E_0}\right) - 1\right\}, \tag{8}$$

where I_{TU0} is the saturation value of the tunneling current component I_{TU}, E_0 is a parameter dependent on barrier transparency. As suggested by Padovani and Strattson [7]:

$$E_0 = E_{00}\coth\left(\frac{E_{00}}{kT}\right), \tag{9}$$

With

$$E_{00} = \frac{qh}{4\pi}\sqrt{\frac{N_D}{\varepsilon_S m_n^*}}, \qquad (10)$$

where ε_S is the dielectric constant.

Finally, the leakage component of the current is

$$I_{LK} = \frac{V - R_s I}{R_t}, \qquad (11)$$

where R_t is the parasite resistance which represents the inhomogeneities and defects at the metal-semiconductor interface.

4. Results and Discussion

In this part we present the different electrical parameters determined from the current-voltage and the capacitance voltage characteristic of the structure Ni/Au/AlInN/GaN.

The gate current Igs (Vgs) of the Ni/Au/AlInN/GaN HEMT is illustrated in Fig. 2. The transistors has a linear characteristic up to 1.5 V, beyond the effect of the series resistance appears.

The saturation current (I_s), barrier height $a(\phi_{bn})$, ideality factor (n) and series resistance (R_s) determined from the characteristic are 3.47×10-10 A, 0.72 eV, 2.3 and 33 Ω, respectively.

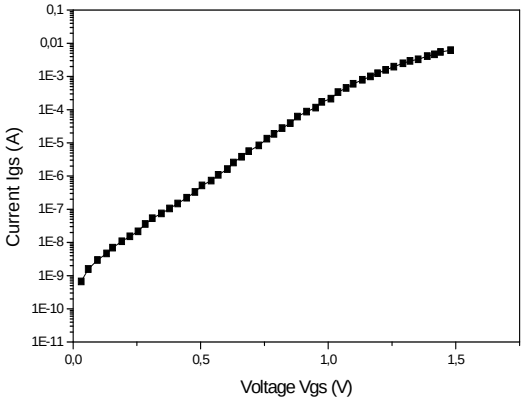

Fig. 2. Gate leakage current $I_{gs}(V_{gs})$ of the HEMT.

According to Card and Rhoderick, for a real Schottky diode having interface states in equilibrium with the semiconductor, the ideality factor n becomes greater than unity and is given by [8-11]:

$$n(V) = 1 + \frac{\delta}{\varepsilon_i}\left(\frac{\varepsilon_s}{W} + qN_{ss}\right), \qquad (12)$$

where N_{ss} is the density of interface states; W is the width of the semiconductor, and ε_i is the permittivity of the interfacial layer. The voltage-dependent ideality factor $n(V)$ can be expressed as

$$n(V) = (q(V - RSI)/(kT \ln(I / I_s))).$$

The expression for the interface state density can be given as:

$$N_{ss} = \frac{1}{q}\left(\frac{\varepsilon_i}{\delta}(n(V)-1) - \frac{\varepsilon_s}{W}\right), \qquad (13)$$

In the n-type semiconductor, the energy of the interface states E_{ss} with respect to the bottom of the conduction band at the surface of the semiconductor is given by [12]:

$$E_c - E_{ss} = q(\phi_{bn} - (V - IR_s)), \qquad (14)$$

The $I(V)$ characteristic in a Schottky diode is used to evaluate the surface state density N_{ss}, Fig. 3 represents the energy density distribution profile of the Au/Ni-AlInN Schottky diode. As can be seen the N_{ss} values obtained taking the series resistance values into account are lower than those obtained without considering the series resistance.

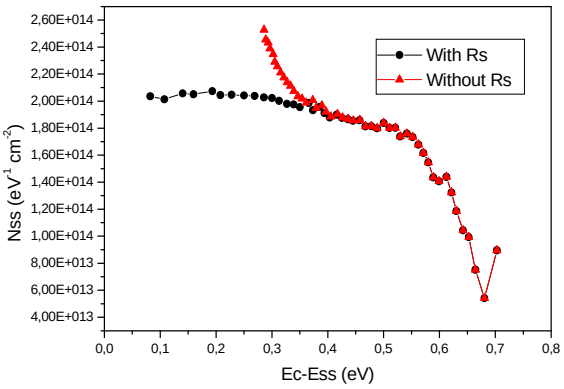

Fig. 3. The energy density distribution profile of the Au/Ni-AlInN Schottky diode.

We note that the density of interface state increases when approaching the conduction band structures for taking into account the series resistance R_s. By cons when we consider this resistance, we observe a saturation zone between E_c-E_{ss} = 0.08 eV and E_c-E_{ss} = 0.31 eV which corresponds to $aN_{ss} \approx 2\times10^{14}eV^{-1}cm^{-2}$. So it may indicate the presence of a deep level in this energy [13].

The energy values of the density distribution of the N_{ss} are in the range E_c-0.285 to E_c-0.68 eV. As can be seen in Fig. 3, the magnitude of the N_{ss} without and with taking into account the R_s in E_c-0.285 eV is 2.52×10^{14} eV^{-1} cm^{-2} and

2.03×10^{14} eV^{-1} cm^{-2}, respectively at room temperature. The N_{ss} values obtained with considering the series resistance are lower than those obtained taking the series resistance values into account. The above explanation shows that the series resistance value should be taken into account in determining the interface state density distribution curves.

Fig. 4 shows the capacitance-voltage characteristic of the Ni/Au/AlInN/GaN HEMT.

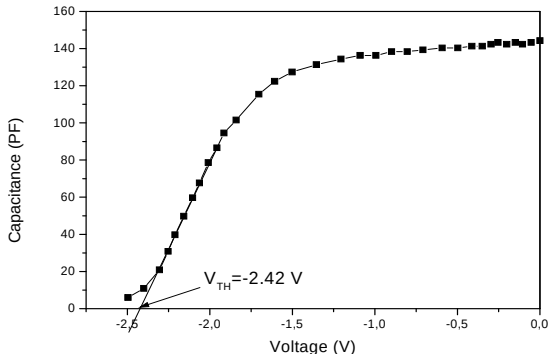

Fig. 4. The capacitance of the AlInN/GaN HEMT.

The threshold voltage VTH (defined by a linear extrapolation of the capacitance curve versus voltage to zero capacitance) is -2.42 V. The 2DEG sheet carrier density n2DEG is given by:

$$n_s = \int \frac{C_{gaz2D^{dv}}}{qA}(V:0-V_{th}), \qquad (15)$$

where q is the electron charge and A is the diode area. The 2DEG sheet carrier density calculated from the C–V curve integration was 1.35×1013 cm-2. We have deduced the carrier concentration profile Nc-v versus the space charge depth W in the heterostructure according to the following relation:

$$\frac{1}{c^2} = \frac{2(V_R + V_0)}{q\varepsilon_r\varepsilon_0 N_D S^2}, \qquad (16)$$

and

$$W = S\frac{\varepsilon_r\varepsilon_0}{c}, \qquad (17)$$

where V_R is the reverse bias voltage; V_0 is the diffusion potential; q is the electronic charge; ε_0 is the free-space dielectric constant; ε_r is the relative dielectric constant of InAlN barrier, and N_D the doping concentration.

The results are plotted in Fig. 5. It exhibits a strong peak of a carrier density equals to 2.41×1021 cm^{-3} corresponding to the presence of a gas (2DEG) at the interface InAlN/GaN. The position of this peak proves that InAlN layer thickness is about 11 nm. In addition, we have determined the net doping concentration ND from the lot of $1/C^2$ as a function of gate voltage. We have found $N_D = 4.6\times1019$ cm^{-3}.

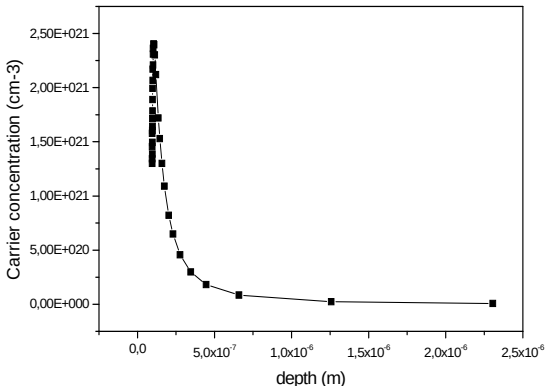

Fig. 5. The carrier concentration profile versus the depth W of the AlInN/GaN HEMT.

The Table 2 summarizes the electrical parameters calculated from characteristic I (V) and C (V) for the structure Ni/Au/AlInN/GaN.

Table 2. The electrical parameters of AlInN/GaN HEMT.

I(V)	I_s (A)	3.47×10^{-10}
	n	2.3
	Φ_{bn} (eV)	0.72
	R_s (Ω)	33
C(V)	V_{th} (V)	-2.42
	N_{2D} (cm^{-3})	1.35×10^{13}

To conclude the experimental part, we find that the AlInN material indicates the presence of a 2D gas larger than the AlGaN material; so this is a promoter material. Remains to improve the technology of metal to minimize the current flows in reverse.

5. Modeling of I (V) Characteristics

As example, the fitting result for the data measured on the Ni/ Au/AlInN/GaN Schottky diodes at room temperature are shown in Fig. 6, a good agreement between the experimental and calculated curves was obtained for the following values R_s = 33 Ω, $R_p = 5\times10^7$ Ω, E_0 = 78 meV with $N_D = 4.6\times10^{19}$ cm^{-3} which corresponds to de doping of de layer GaN and V_d = 1.11 V.

Fig. 7 shows the experimental and theoretical characteristic I(V) according to the contribution of each current.

An impact of the individual current components can be summarized as follows:

- The thermionic current is significantly lower than the measured total current, mainly at lower bias voltage.
- The generation-recombination current can be neglected for all bias voltage used.

- The tunneling current dominated for the entire range of polarization.
- The leakage current can be observed for voltage lower than 0.25 V.

These results support an assumption that the dominant current mechanism in Ni/Au/AlInN/GaN Schottky diodes is the tunneling current governed by dislocations.

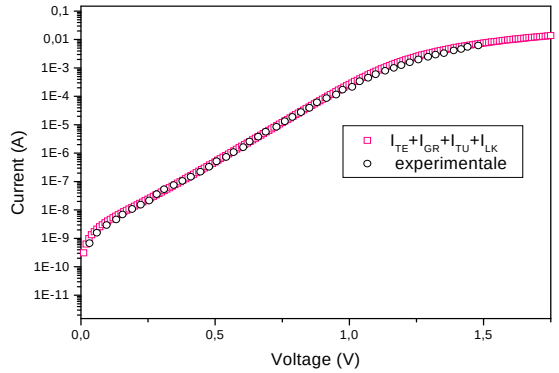

Fig. 6. Characteristics I(V) experimental and theoretical of the Ni/Au/AlInN/GaN structure.

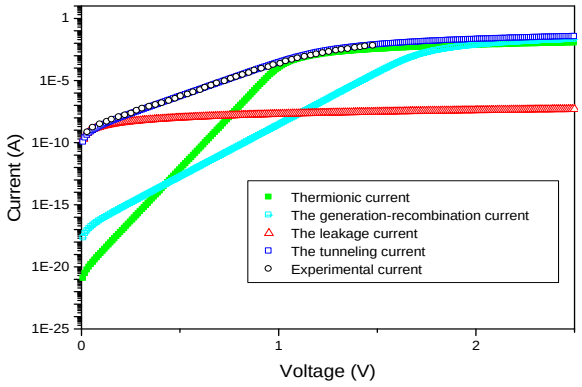

Fig. 7. Characteristics I(V) following experimental and theoretical contribution of each current of the Ni/Au/AlInN/GaN structure.

6. Conclusion

In summary, we have investigated measurements on AlInN/GaN grown by LPMOCVD current–voltage characteristics; We have studied the Schottky contact of Ni/Au/AlInN/GaN transistor. The current–voltage Igs(Vgs) of Ni/Au/AlInN/GaN structure were investigated at room temperature. The AlInN HEMT has a reverse current ($I = 3.47\times10^{-5}$A). The electrical parameters such as ideality factor (2.3), barrier height (0.72 eV) and series resistance (33 Ω) were evaluated from I–V data. The value of the density of gas evolved from the curve C (V) is of the order of (1.35×1013 cm^{-2}). The characterization and modeling *I*(*V*) of the gate Schottky structures have been analyzed and discussed.

References

[1]. A. Gadanecz, J. Bläsing, A. Dadgar, C. Hums, and A. Krost, Thermal stability of metal organic vapor phase epitaxy grown AlInN, *Applied Physics Letters,* 90, 2007, pp. 221906-221909.

[2]. J. Kuzmík, A. Kostopoulos, G. Konstantinidis, J. F. Carlin, A. Georgakilas and Pogany, InAlN/GaN HEMTs: a first insight into technological optimization, *IEEE Transactions on Electron Devices*, Vol. 53, 2006, pp. 422-426.

[3]. J. Kuzmík, Power electronics on InAlN/(In)GaN: Prospect for a record performance, *IEEE Electron Device Letters*, Vol. 22, 2001, pp. 510–512.

[4]. F. Medjdoub, J. F. Carlin, C. Gaquière, N. Grandjean, and E. Kohn, Status of the emerging InAlN/GaN power HEMT technology, *Open Electrical and Electronic Engineering Journal*, Vol. 2, 2008, pp. 1–7.

[5]. H. C. Card, E. H. Rhoderick, Studies of tunnel MOS diodes II. Thermal equilibrium considerations, *Journal of Physics D: Applied Physics*, Vol. 4, 1971, pp. 1602-1606.

[6]. B. J. Baliga, Modern Power Devices, *Wiley*, New York, 1987.

[7]. F. A. Padovani, R. Straton, Field and Thermionic-Field. Emission in Schottky Barriers, *Solid States Electronic*, Vol. 9, 1966, pp. 695-707.

[8]. H. C. Card, E. H. Rhoderick, Studies of tunnel MOS diodes I : Interface effects in silicon Schottky diodes, *of Physics D: Applied Physics*, Vol. 4, 1971, pp. 1589-1601.

[9]. S. Altındal, H. Kanbur, I. Yücedag, A. Tataroglu, Sur la distribution d'énergie des états d'interface et leur temps de relaxation et de capturer des profils de section transversale en Al/SiO2/Si-p diodes Schottky (MIS), *Microelectronic Engineering*, Vol. 85, 2008, pp. 1495-1501.

[10]. F. Parlaktürk, S. Altındal, A. Tataroglu, M. Parlak, A. Agasiev, On the profile of frequency dependent series resistance and surface states in Au/Bi4Ti3O12/SiO2/n-Si(MFIS) structures, *Microelectronic Engineering*, Vol. 85, 2008, pp. 81-88.

[11]. S¸ Altındal, H. Kanbur, A. Tataroglu, M.M. Bülbül, The barrier height distribution in identically prepared Al/p-Si Schottky diodes with the native interfacial insulator layer (SiO2), *Physica B: Condensed Matter*, Vol. 399, 2007, pp. 146-154.

[12]. M. K. Hudait, S. B. Krupanidhi, Interface states density distribution in Au/n-GaAs Schottky diodes on n-Ge and n-GaAs substrates, *Materials Science* and *Engineering B*, Vol. 87, 2001, pp. 141-147.

[13]. W. Chikhaoui, J.-M. Bluet, M.-A. Poisson, N. Sarazin, C. Dua, and C. Bru-Chevallier, Current deep level transient spectroscopy analysis of AlInN/GaN high electron mobility transistors: Mechanism of gate leakage, *Applied Physics Letters*, Vol. 96, 2010, pp. 072107-1- 072107-3.